The Muon Portal project: a dedicated muon detector for the inspection of shipping containers

U. Becciani*, V. Antonuccio*, M. Bandieramonte*†, F. Belluomo‖
M. Belluso*, S. Billotta*, D.L. Bonanno†, G. Bonanno*, A. Costa*,
G. Fallica§, S. Garozzo*, V. Indelicato†, P. LaRocca†‡, E. Leonora‡, F. Longhitano‡,
S. Longo¶, D. Lo Presti†‡, P. Massimino*, C. Petta†‡, C. Pistagna*, C. Pugliatti†‡,
M. Puglisi‖ N. Randazzo‡, F. Riggi†‡, S. Riggi*, G. Romeo*, G.V. Russo†‡, G. Santagati†‡,
G. Valvo§, F. Vitello*, A. Zaia¶, G. Zappalà†
*INAF - Osservatorio Astrofisico di Catania, Italy
†Dipartimento di Fisica e Astronomia - Catania, Italy
‡INFN - Catania, Italy
§STMicroelectronics - Catania, Italy
¶Insirio - Messina, Italy
‖Meridionale Impianti Welding Technology - Catania, Italy

***Abstract*—Traditional techniques, such as those based on X-rays absorption, to inspect shipping container in search of potential fissile threats cannot be employed on occupied vehicles and are of limited use in presence of a large amount of shielding materials. To overcome such limitations, prototypes of detection systems employing the muon tomography technique, based on cosmic muon scattering from high-Z materials, are being tested worldwide. The Muon Portal project aims to build a large area muon detector (18 m^2) for the inspection of TEU containers with good spatial and angular resolution. The detector is made by four XY tracking planes of plastic scintillator bars with embedded WLS fibers and SiPM readout, placed above and below the volume to be inspected. Different imaging and visualization algorithms are being designed and tested over tomographic scenarios simulated with a detailed software replica of the entire detector. Experimental tests of the individual detection modules are already in progress. The design and operational parameters of the portal under construction are reported, together with the preliminary detector tests and imaging results.**

I. Introduction

Each year hundred million vehicles, transporting persons and materials, cross the custom borders of many Countries. All of them are capable of transporting small quantities of hidden nuclear material, such as fissile elements. Traditional systems based on X-ray inspection cannot be employed on occupied vehicles, since the energy or dose required would be too high in order to penetrate big cargos and result in a significant image of the hidden volume. As an alternative to traditional detection methods, it has been long suggested to employ the scattering process of the secondary cosmic radiation at the sea level (mainly muons), which strongly depends on the atomic number of the traversed material, hence particularly sensitive to high-Z fissile elements (U, Pu) or their shielding. A detection system employing such technique (muon tomograph) would require a large area muon detector, to reconstruct the muon tracks with good angular resolution, before and after their passage through the volume. Proper algorithms need to be applied to produce a tomographic image of the container volume, able to signal the presence of hidden, high-Z materials.

Due to the natural flux of secondary cosmic muons at the sea level, enough muon tracks are expected to cross the large volume of a container (in the order of 50 m^3 for a 20' container) in a reasonable amount of time (few minutes), thus producing enough collected events to reconstruct a tomographic image with good precision.

Different Projects have been proposed over the past years, aiming at building prototype detectors for muon tomography [1], [2], [3]. They differ in the sensitive area and in the details of the detection technique employed. A new Project was recently started by the Muon Portal Collaboration [4] with the goal to build a real size detector (18 m^2 sensitive area) with all potential features to be used in a real situation to probe the interior of a standard container. The main parameters of the design of such setup, together with the instrumentation required, are here described. A considerable amount of simulations and tests with different reconstruction and visualization algorithms has demonstrated the feasibility of this Project and the possibility of reaching enough information in a reasonable amount of time to reconstruct the tomographic image with the required precision and resolution. Experimental tests for the construction of the first detection modules are in progress, and most of the technical solutions concerning detectors, photosensors, front-end electronics, data acquisition, reconstruction and visualization have been already fixed. Preliminary descriptions of such Project have been previously reported [5], [6].

II. The Muon Portal Detector

A. Geometrical and mechanical structure

The structure of the detection setup is based on eight position-sensitive physical planes (corresponding to four logical XY planes). Two logical planes are placed above and two planes below the container volume to be inspected (see Fig. 1). Due to the envisaged distances between the detection planes (100-140 cm) and the inner part of the detector (about 300 cm height, to allow the insertion of a standard container), a good

978-1-4799-1535-4/13/$31.00 ©2013 IEEE

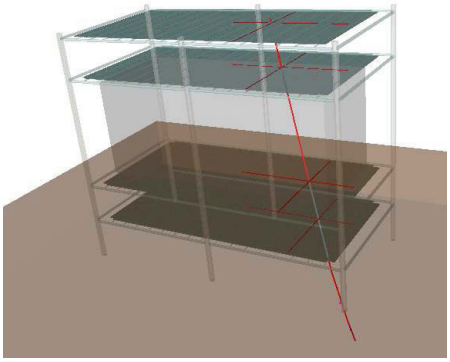

Fig. 1. A sketched view of a Muon Tomograph. Two XY logical detection planes are placed above and below the container at a relative distance of the order of 100 cm, in order to reconstruct the muon tracks before and after traversing the container volume, searching for muon scattering from high-Z objects.

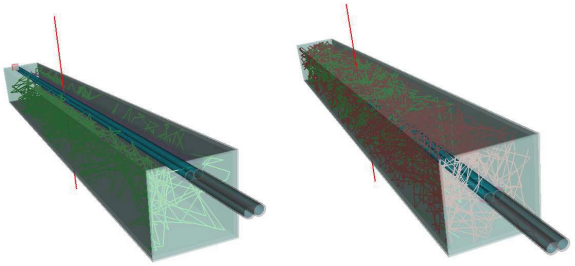

(a) Amcrys design (b) Fermilab design

Fig. 2. Two among the various designs of the extruded scintillator strips, together with typical GEANT4 simulated events generated by the passage of cosmic muons, with optical photons being transported inside the detector.

spatial resolution, in the order of a few mm, is required for all planes, in order to provide good tracking capabilities for the incoming charged particles, reconstruct their trajectories before and after the container and evaluate the amount of scattering suffered by each track.

The overall size of the detector fits that of a real TEU (Twenty-foot Equivalent Units) container, namely 6 m $\times$ 3 m $\times$ 3 m. For a suitable implementation of the detection setup, each plane is made by 6 modules (1 m$\times$3 m each) in a proper geometry, such as to cover both the X- and the Y-coordinates by the same type of modules, without leaving any dead area.

A customized mechanical structure has been designed, to provide a suitable support for the detector planes, yet minimizing the material budget traversed by the cosmic muons. Mechanical stress due to the weight of the various components and to temperature variations has been investigated, together with the alignment problems when mounting the detection modules.

B. Strip and module design

Each detection module is segmented into 100 strips of extruded plastic scintillator ($1\times1\times300$ cm^3), with wavelength-shifting (WLS) fibres to transport the light produced in the scintillator to the photosensors placed at one of the fibre ends.

A series of experimental tests have been carried out on several prototypes of scintillator strips and WLS fibres from different suppliers, in order to choose the configuration for the final design of the detector, and optimize the light collection at one end of the strip. Among the strip prototypes with 1 cm^2 cross section, we tested various samples of strips with a centered hole able to accomodate two 1 mm WLS fibres (Fermilab design) as well as strips with two 1 mm holes put on the same side (Amcrys design). Figure 2 shows such possible design for the two strips.

The setup employed for such tests included a dark box with the strip, fibres and SiPM readout modules, together with two opposite small-area scintillators to define a region along the strip, where to measure the light yield detected for each SiPM. GEANT4 simulations of the transport of optical photons inside the scintillator strips and the WLS fibres have been carried out for each geometrical configuration.

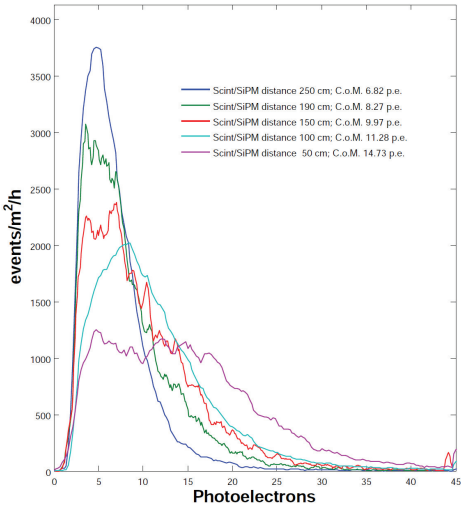

Fig. 3. Comparison between spectra of the light yield obtained at different distances along the strip, with a 3 m long WLS fibre.

Fig. 3 shows a comparison between the spectra obtained at various distance (50-250 cm) from the SiPM. Since the threshold can be safely put at 2 p.e., a good uniformity along the strip may be expected.

A design of the individual detection module (100 strips, 1 m $\times$ 3 m) has been already prepared and an assembly tool is being built, to pack the strips, insert the WLS fibres, prepare their surface with a diamond tool for an optimal optical coupling to the photosensors and arrange the connection to the front-end electronics at one end of the module.

C. Photo-sensor design

For the readout of the scintillation light produced in the strips and transported by the WLS fibres, Silicon photo-multipliers are being used. Different SiPM technologies are currently developed and tested by STMicroelectronics, which is one of the industrial partner of the Project. The goal of such activity is to arrive at the production of devices with a high photon detection efficiency (PDE), a high fill factor, and a low cross-talk. At the moment, several prototypes, both with the p/n and n/p technologies, have been produced. The prototype being considered for this application is a 1.5 $\times$1.5 mm^2 device, with 625 cells (size 60×60 μm^2), and a fill factor of about 67

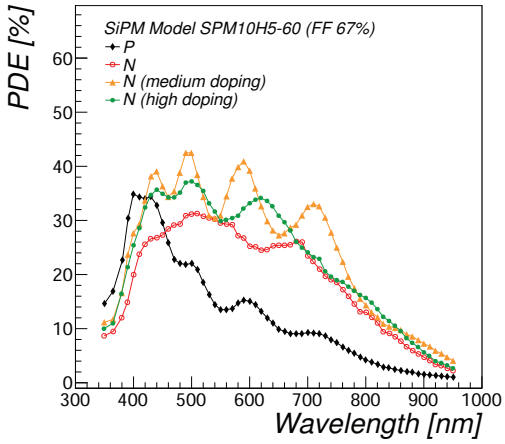

Fig. 4. Measurements of the Photo Detection Efficiency (PDE) as a function of wavelength for different Silicon photomultipliers technologies designed by STMicroelectronics for the Muon Portal detector.

%.

Fig. 4 shows a summary of PDE laboratory measurements carried out at different wavelengths on several SiPM devices designed with different technologies for an overvoltage of 5 V. An intense work of characterization of such devices, both from the electrical and optical point of view has been made, at different temperatures and operating conditions, also making use of digital pulse processors. Simulations of the devices under development are also being considered and comparison of the data with Monte Carlo and SPICE calculations have been carried out to improve the SiPM design.

D. Electronic readout and data acquisition

Taking into account the number of modules and the required granularity to achieve a reasonable space and angular resolution, a large number of channels is required. A compression technique within each module (100 strips) is envisaged in our Project, which reduces such number to a suitable level for the electronics and data acquisition. This is achieved by the use of two WLS fibres running along the same strip (for a total of 9600 WLS fibres) and going to an equal number of SiPMs. The logical output from different photosensors is then properly combined in groups of ten, resulting in 20 channels per module. Their combination is able to identify the interested strips inside each module.

The front-end electronics is based on the use of MAROC3 chips (64 channels each), which have an adjustable gain (channel-by-channel), a fast shaping and a common threshold. Real-time boards based on FPGA FlexRIO are being used, with a sampling rate up to 250 MHz.

For the purpose of correlating the arrival of muons in the Muon Portal detector to additional detectors located around it, a GPS time-stamping unit is also planned in the acquisition architecture. This will allow off-line correlation of the events measured in independent detectors, with a time precision of about 40 ns.

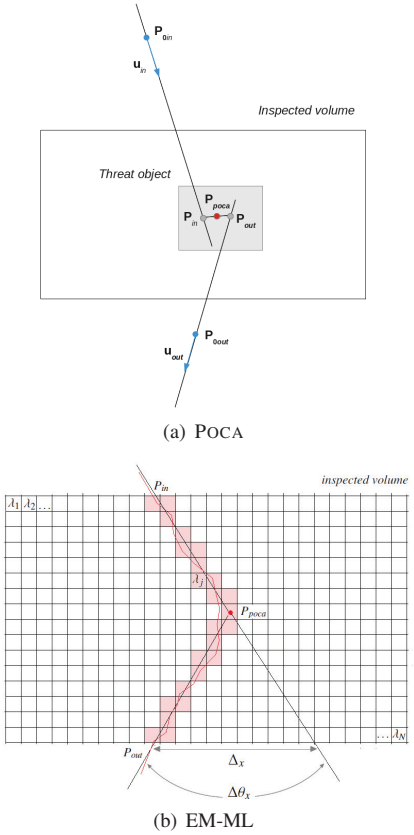

Fig. 5. A sketch illustrating the working principle of the POCA (III) and EM-ML (III) methods.

III. MUON TOMOGRAPHY IMAGING

A. Imaging methods

Several algorithms have been tested for the reconstruction of target objects located inside the container volume. The simplest of them is based on the POCA (Point-of-Closest-Approach) method, from which a spatial distribution of the scattering centres is derived, with a weight proportional to some power of the scattering angle.

The algorithm makes the simplified assumption that the muon scattering occurs in a single-point. It therefore searches for the geometrical point of closest approach $\mathbf{P}_{poca}$=$\frac{1}{2}(\mathbf{P}_{in} + \mathbf{P}_{out})$ between the incoming $\mathbf{u}_{in}$ and outcoming $\mathbf{u}_{out}$ reconstructed track directions with respect to the inspected volume (see sketch in Fig. III):

$$\mathbf{P}_{in,out} = \mathbf{P}_{\mathbf{o}\,in,out} + t_{in,out}\mathbf{u}_{in,out} \quad (1)$$

$$t_{in} = (be - cd)/\Delta \quad (2)$$

$$t_{out} = (ae - bd)/\Delta \quad (3)$$

where $\mathbf{P}_{\mathbf{o}\,in,out}$ are two points on the incoming and outgoing tracks, $a = \mathbf{u}_{in}\cdot\mathbf{u}_{in}$, $b = \mathbf{u}_{in}\cdot\mathbf{u}_{out}$, $c = \mathbf{u}_{out}\cdot\mathbf{u}_{out}$, $d = \mathbf{u}_{in}\cdot\mathbf{w}$, $e = \mathbf{u}_{out}\cdot\mathbf{w}$, $\Delta = ac - b^2$, $w = \mathbf{P}_{\mathbf{o}\,in} - \mathbf{P}_{\mathbf{o}\,out}$.

We implemented different statistical methods to analyze the distribution of the POCA scattering points, which are presented in detail in [7]. Some of them makes use of three-dimensional grids to bin the spatial POCA data and considers the significance of count excess observed in each cell with

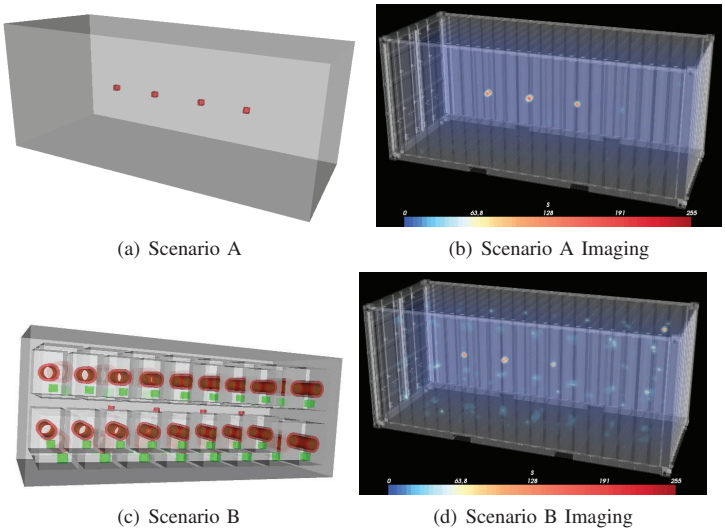

(a) Scenario A (b) Scenario A Imaging

(c) Scenario B (d) Scenario B Imaging

Fig. 6. Simulated tomographic scenarios (left panels) and 3D volume rendering of the EM-ML imaged scenarios (right panels).

respect to the expected background as a criterion for the target identification. Other methods tested are grid-free, such as the two-points autocorrelation analysis and density-based clustering algorithms.

POCA-based methods, although of easy implementation, neglect the multiple scattering through the volume material and therefore have the drawback of providing poor-resolution images, they are quite sensitive to the presence of shield materials located above or below the potential threat and cannot localize very well materials at the volume borders.

A better physical and statistical treatment of the scattering processes can be done using a maximum likelihood method, hereafter denoted as the EM-ML method. It assumes the container volume to be imaged divided into N_{voxels} three-dimensional voxels, each with unknown scattering density λ_j (see sketch in Fig. III), defined by:

$$\lambda_j = \left(\frac{15 \text{ MeV}}{p_0} \right)^2 \frac{1}{L_{rad}} \tag{4}$$

where p_0 is the muon momentum and L_{rad} is the radiation length of the traversed material. The scattering densities λ_j (j=1,... N_{voxels}) for each voxel can be determined by fitting the scattering data $\mathbf{x}_i$=($\Delta\theta_{x,y}$, $\Delta_{x,y}$) for each i-th muon event for both x and y coordinates. An efficient fitting strategy is given by the Expectation-Maximization (EM) algorithm which provides an iterative solution for the λ_j, see for instance [8].

B. Application to simulated data

A full GEANT4 replica of the complete detector has been implemented, incorporating the individual scintillator strips, the mechanical structure, the walls of the container, together with the soil below the detector. In each particular simulation, a set of objects of low-, medium- and high-Z material may be placed by the user inside the container volume, to understand the effect on the muon scattering and probe the capabilities of the reconstruction algorithms.

Secondary cosmic particles (muons and electrons) are modelled with realistic energy and angular distributions, as derived from CORSIKA simulations for proton-induced showers, taking into account the primary energy and angular distribution. In order to save CPU time, the transport of optical photons inside the scintillator strips and WLS fibres has been simulated in detail for a particular strip and then parameterized to take into account the response of the overall detector.

The reconstruction of the events simulated in the detector proceeds through the following stages. The hits obtained in each detection plane are first collected and possible clusters are searched and identified. For both upper and lower detection planes, the muon track is reconstructed either by using a Least-Square approach or a Kalman Filter approach. Finally, the scattering data, scattering angles and lateral displacements, are estimated from the obtained tracks in upper and lower planes and passed to the imaging stage.

We validated the developed tomography algorithms over several simulated scenarios. In Fig. 6 we report two sample scenarios, denoted as scenario A and B, imaged with the EM-ML method. The first scenario is made by four threat boxes of different materials (W, U, Pb, Sn) of size 10 cm$\times$10 cm$\times$10 cm inserted at the center of an empty container. The second scenario assumes the same threats box inserted in a denser environment, filled with layers of washing machine-like elements, made by an aluminium casing with an iron engine inside with relative support bars and a concrete block. A number of 5×10^5 muon events has been simulated for both scenarios using a realistic energy spectrum with range 0.1-100 GeV.

As it can be seen, both scenarios are successfully identified. A considerable noise, related to the engine elements, is present in the dense environment scenario. POCA-based algorithms provide alternative results, with a slightly worse imaging resolution due to a persistent halo around the target objects.

At present, we are putting large efforts to optimize the developed methods (i.e. computation times, performances and so forth) and to perform statistical studies with the aim of determining the expected detection efficiencies and rate of fake identification of the tomograph.

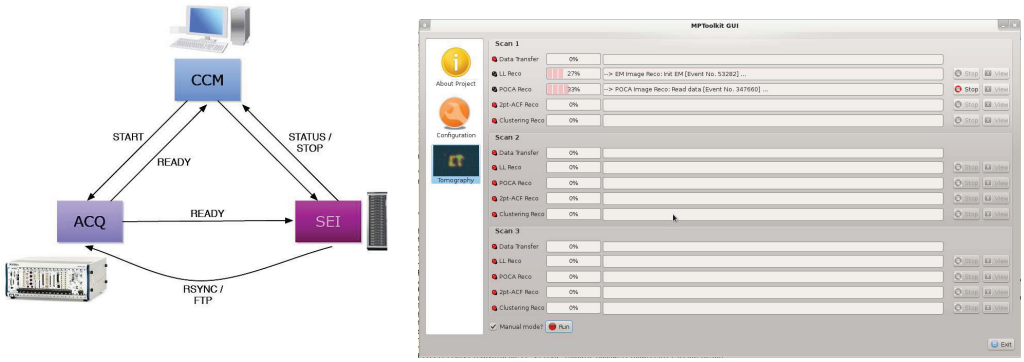

(a) Communication schema (b) Online tomography panel

Fig. 7. 7(a): Schema of inter-communication between all available devices installed in the Muon Portal project for the online tomography imaging; 7(b): A view of the GUI panel available for the online tomography imaging.

IV. The elaboration and monitoring system

In view of the full operation of the portal, we foreseen the development of an image elaboration system and a control and monitoring system. The former is responsible for the processing of tomography analysis, image visualization and storage and alarm identification. The latter is designed for control of the data acquisition procedures (i.e. run start/stop, calibration modes, and so on) and for collecting, handling and storing the monitoring observables generated from different devices in the portal.

A sketch of the prototyped system and its working schema is shown in Fig. 7(a). The imaging elaboration system (SEI) is made up of a set of computing machines (24 cores in our preliminary design) and connected through a local LAN network to the data acquisition crate (ACQ) and the controller machine (CCM). The CCM send a start message to the ACQ that initiate the data acquisition and at the same time also to SEI to inform of the current status. After a prespecified scanning time the ACQ produced the first bunch of raw data and send a ready message to SEI, that, on message receive, starts transferring the raw data and the image elaboration. At elaboration finished, with or without an alarm status, SEI communicates the status of the image processing to the CCM. The above procedure is planned to be repeated in cases of an alarm status.

The communication from/to the CCM and ACQ machines is effectively realized by exchanging structured messages in JSON format [1] respectively using webservice and TCP/IP socket protocols in a simple server/client strategy.

At the present status, the image elaboration system is at an advanced stage, while the monitoring system is under development. We developed a Qt-based GUI (see a screenshot in Fig. 7(b)) which provide an an easy and fully customization of the tomography algorithm for non-expert users, allows to perform in real-time the tomography analysis either in a manual or driven mode. A 3D viewer, based on Qt+Vtk, has been also implemented for real-time visualization (volume renderings, tomographic planes, isosurface extraction and so on).

[1] Typical messages exchanged contains univoquely identifiers for the container under scan, command directives to be executed and so forth.

V. Present status of the Project and outlook

For the overall completion of this Project, a preliminary research and development phase has been undertaken on several aspects which jointly contribute to the final design and construction of the prototype: the optimization of the individual detectors and their working conditions, the characterization of the optical photosensors and their coupling to the scintillator strips and WLS fibres, the design of the software algorithms for track reconstruction and image processing. Prototypes of SiPM sensors have been already produced by the STMicroelectronics and will be customized for this specific application. The geometry and segmentation of the strip detectors is already finalized, with most of the preliminary tests already carried out. The architecture of the front-end electronics and of the data acquisition has been designed and the first modules are under construction. All the simulation and reconstruction tools have been tested, and only minor improvements and optimization required.

Such $R\&D$ phase will soon be followed by the construction of the overall apparatus (48 modules, for a total of 4800 detectors), in order to arrive at the completion of the entire setup, within the end of 2014, and carry out all the necessary calibration measurements and data analysis, which are a particularly important and critical step towards the real use of the apparatus.

Due to the large acceptance of the detector for cosmic rays, complemented by a good angular reconstruction of the muon tracks and possibility to discriminate electrons from muon events, it is also planned to employ such detector for cosmic ray studies. For such applications in cosmic ray physics the muon detection capabilities will be complemented by a set of trigger detectors located some distance apart with respect to the Muon Tomograph, in order to measure multiple muon events (muon bundles) associated to extensive air showers.

References

[1] Borozdin K R 2003 *Nature* **422** 277
[2] Gnanvo K et al 2011 *Nucl. Instr. and Meth.* A **652** 16
[3] Pesente S et al 2009 *Nucl. Instr. and Meth.* A **604** 738
[4] For further details visit our Web site: *http://muoni.oact.inaf.it*

[5] S.Riggi et al. (The Muon Portal Collaboration), Proceedings of the ECRS 2012 Conference, Moscow, 3-7 July, 2012, J.Phys.G(Conf.Series)**409**(2012)012046.

[6] D.Lo Presti et al. (The Muon Portal Collaboration), Proceedings of the IEEE Nuclear Science Symposium and Medical Imaging Conference (NSS/MIC), Anaheim, Oct.27-Nov.3, 2012.

[7] S.Riggi et al. (The Muon Portal Collaboration), Nuclear Instruments and Methods, submitted.

[8] Schulz L J et al 2007 *IEEE Transactions on Image Processing* **16** 8